Journal of Molecular Biology and Molecular Imaging

Open Access

Austin Publishing Group

Rapid Communication

Addressing the Challenges of Multi-Immunofluorescent Deep Tissue Imaging of Islets and Vasculature in the Rat Pancreas

Naidoo V, Lang DM and Van der Merwe EL*
Department of Human Biology, University of Cape Town, South Africa

***Corresponding author:** Van der Merwe EL; Department of Human Biology, University of Cape Town, Faculty of Health Sciences, Private Bag, Observatory, 7935, South Africa

Received: November 15, 2015; **Accepted:** December 03, 2015; **Published:** December 07, 2015

Abstract

Whilst whole-mount (WM) multi-immunofluorescence is useful for studying selected micro anatomical relationships in three dimensions, our studies on pancreatic tissues revealed that signals of different fluorophores for localizing distinct structures were not equally detectable at all optical planes. We thus sought to determine the underlying reasons for this observation. Multiple fluorophores covering the blue to far red emission spectra were used to detect islets (insulin - AMCA/Cy2/Cy3) and pancreatic vasculature (*Lycopersicon esculentum* lectin-FITC, Collagen IV/Cy5, α-SMA/Alexa Fluor®488 or α-SMA/Alexa Fluor®647). Regardless of antibody concentration or mountant, insulin was only detectable up to ≈66μM with AMCA. Nuclei stained by Hoechst 33342 were detected deeper (≈130μM), suggesting that internal absorption was unlikely the main reason for the poor detectability of AMCA. By contrast, insulin/Cy2 was detectable much deeper in WMs mounted in methyl salicylate (maximum ≈300μM), but many of these islets showed stronger staining on the superficial plane than seen internally. Insulin/Cy2 islets were barely detectable in glycerol (GL). Collagen IV/Cy5 detected vasculature at deeper planes in salicylate, more so than some of the aforementioned antibodies/fluorophores for vasculature detection, but the grainy resolution meant it was unsuitable for future experiments. By contrast, insulin/Cy3and lectin-FITC were readily detectable in both mountants but more superior image quality was shown in glycerol-mounted tissues at deeper optical planes (maximum ≈213μM). We thus conclude that insulin/Cy3 and lectin-FITC provided the most promising antibody combination for detectability and resolution of insulin in β-cells in islets and vasculature, respectively, down to ≈200μM in the WMs.

Keywords: 3-D imaging; Multi-immunofluorescence; Deep tissue imaging; Islets; Fluorophores; Optical clearing

Abbreviations

3-D: Three-dimensional; α-SMA: Alpha-Smooth Muscle Actin; AMCA: Aminomethylcoumarin Acetate; β-cells: Beta cells; BSA: Bovine Serum Albumin; CLSM: Confocal Laser Scanning Microscope; Cy: Cyanine; DABCO: 1,4-Diazabicyclo[2.2.2]octane; DPSS: Diode-pumped Solid-State; ECRA: Ethics Committee for Research on Animals; GL: Glycerol; GP: Guinea Pig; HeNe: Helium Neon; hr: hours; JIR: Jackson Immuno Research; Lectin-FITC: *Lycopersicon esculentum* Lectin-FITC; min: minutes; nm: Nanometer; NA: Numerical Aperture; PBS: Phosphate Buffered Saline; PFA: Paraformaldehyde; SAL: Methyl Salicylate; SA MRC: South African Medical Research Council; TX-100: Triton X-100; WEM: Wide-field Epifluorescence Microscopy; WM: Whole-Mount; viz.: Namely; μM: Micron

Introduction

Multiple immunofluorescent staining and 3-D imaging of pancreatic whole-mounts (WMs) has gained popularity for better understanding of the micro-anatomical and cellular relationships relating to the islet neurovascular complexes [1-9]. Despite the promise of this approach, our studies on multi-immunostained rat pancreatic WMs revealed that not all immunostained structures of interest are equally detectable at optical planes deeper in the tissue. For our studies, we needed to locate islets in WMs under wide-field epifluorescence microscopy (WEM) before progressing to confocal imaging. Because we expected insulin content to be abundant in β-cells in the normal pancreas, we chose to detect islets using AMCA-conjugated secondary antibodies. The capillary network and other antigens of interest would thus be detected with Lectin-FITC and Cy3/Cy5/Alexa Fluor®488/Alexa Fluor®647-conjugated secondary antibodies respectively. Possible reasons that could account for the differential detection of fluorophores on structures known to be present at the deeper planes in the tissue are: insufficient permeabilization and antibody concentrations [10,11]; insufficient antibody incubation periods; weak-emitting fluorophores and antibodies that degrade over time [12]; internal absorption of shorter emission wavelengths due to refractive properties of the tissue (Table 1) [13]; the effect of mounting media (polar vs. non-polar), pH and optical clarity of the tissue on signal brightness [13,14]; and the size of antibody-fluorophore conjugates which may lead to steric hindrance or differences in penetration rate into the tissue. This

Citation: Naidoo V, Lang DM and Van der Merwe EL. Addressing the Challenges of Multi-Immunofluorescent Deep Tissue Imaging of Islets and Vasculature in the Rat Pancreas. J Mol Biol & Mol Imaging. 2015; 2(2): 1022.

Table 1: Excitation and emission wavelengths of fluorophores used; relative brightness of fluorophores.

Fluorophore	Excitation (nm)	Emission (nm)	Relative brightness*
AMCA / Hoechst 33342	345-350 / 350	440-461 / 461	Unknown
FITC / Cy2 / Alexa Fluor®488	495 / 492 / 495	519 / 510 / 519	2 / unknown / 3
Cy3	550	570	1
Cy5 / Alexa Fluor®647	650	668	4; 5

Info available from https://www.jacksonimmuno.com/technical/products/conjugate-selection.
*1 =very bright; 5 =weak but detectable signal [6].

Table 2: Antibodies and fluorophores used in this study.

	Primary Antibody/ Glycoconjugate/ Fluorophore	Antigen/ molecular structure recognized	Original concentration (and dilution)	Company	Catalogue Number
Primary Antibody	GP Anti-Insulin	Insulin/islet	0.2mg/ml (1:100)	Abcam	ab7842
	Rabbit Anti-Collagen IV	Basement membrane in vasculature	1.0 mg/ml (1:500)	Abcam	ab19808
	Mouse Anti-α-SMA	Smooth muscle actin	0.2mg/ml (1:100)	Abcam	ab7817
Glycoconjugate	Lectin-FITC (Fluorescein-*Lycopersicon Esculentum*)	Endothelial cellsin vasculature	2mg/ml (1:160)	Vector Laboratories	X0126
Fluorophore conjugated secondary antibodies	AMCA Donkey Anti-GP	GP Anti-Insulin	1.5mg/ml (1:20; 1:50; 1:100; 1:200)	JIR	108739
	Cy2 Donkey Anti-GP	GP Anti-Insulin	1.4mg/ml (1:200)	JIR	110036
	Cy3 Donkey Anti-GP	GP Anti-Insulin	1.5mg/ml (1:1000)	JIR	102348
	Cy5 Donkey Anti-Rabbit	Rabbit Anti-Collagen IV	1.5mg/ml (1:500)	JIR	111904
	Alexa Fluor®488 Donkey Anti-Mouse	Mouse Anti-α-SMA	1.5mg/ml (1:500)	JIR	113082
	Alexa Fluor®647 Donkey Anti-Mouse	Mouse Anti-α-SMA	1.5mg/ml (1:500)	JIR	715-605-150

JIR – Jackson Immuno Research Laboratories.

study attempts to address several of the above challenges, focussing on the ability to detect pancreatic islets by WEM, and examine islet vasculature (capillaries and mural cells) using different combinations of fluorophores taking into consideration the abundance of the target antigens and the relative brightness of fluorophores.

Materials and Methods

Pancreatic tissues were harvested from Wistar rats as part of ongoing research in our laboratory, (ethics approval: SA MRC ECRA (code 02/11)). All tissues were previously fixed in 4% PFA overnight and stored in 100% methanol at -20°C.

Whole-mount multi-Immunostaining

Tissues were prepared as ≈300μM thick sections (using a McllIwain chopper), blocked over night in 3% BSA in PBS containing TX-100 (see below) and incubated in primary antibody and secondary antibody cocktails (Table 2) for several days each, with continuous gentle agitation at 4°C. TX-100 concentrations of 0.01%, 0.05%, 0.1% and 0.5% were included in the blocking/antibody buffer to determine the effect of detergent concentration on antibody penetration and in reduction of background fluorescence. Tissues were mounted either in PBS/glycerol (GL) containing the anti-fade agent DABCO or in methyl salicylate (SAL). All samples were stored in mountant for at least 48 hr before viewing and imaging.

Imaging

WEM and confocal imaging was done on a Zeiss LSM 510 Meta CLSM (Carl Zeiss, Germany). WEM was used to find islets, and tile scans of the WMs were captured with an AxioCAM camera system. For CLSM imaging, the maximum depth of the signal below the surface of the WMs was determined by setting the range of the Z-stack starting at the surface of the WM, and ending in the focal plane where the fluorescence signal in each channel was no longer detectable. The gain was increased progressively through the Z-stack to improve detection of signals in the deeper planes. Optical sections (separated by 4.5μm intervals) were collected using a dry 20X objective lens (NA 0.8). The following lasers were used: two-photon Mai Tai, Argon, DPSS and HeNe with excitation wavelengths of 750nm, 488nm, 561nm and 633nm respectively. Laser power was also varied to improve detectability of some weaker fluorophores where necessary.

Results

Effect of TX-100 concentrations on signal to background

Insufficient permeabilization of tissues could limit the access of antibodies to intra-cellular antigens and structures deeper in the tissue. We used Lectin-FITC staining of the vasculature (as this is prevalent throughout the pancreas) to determine the effect of detergent concentration on signal intensity. The depth at which Lectin-FITC signals were detectable was greater in WMs treated with 0.01% and 0.1% TX-100 (Figure 1, Table 3) compared to the other concentrations. The best contrast between signal and background was shown in 0.1% TX-100 (Figure 1).

Insulin detection using fluorophores emitting in the blue, green and red emission spectra

Fluorescence of is lets stained by insulin/AMCA was very poor (Figure 2A). Despite increasing the AMCA concentration from 7.5μg/ml to 75μg/ml, using a different batch of AMCA-labelled secondary

Table 3: Detection of *Lycopersicon esculentum* lectin (Lectin-FITC) at different concentrations of TX-100.

	Triton X-100 (TX-100) concentrations			
	0.01%	**0.05%**	**0.1%**	**0.5%**
Maximum depth of Lectin-FITC detection (μM; n = 6)	106.89	91.62	106.89	81.44

Table 4: Depths of detection of fluorophores used in this study.

Antibody/Fluorophore Combination	Maximum Depth in GL (μM)	Maximum Depth in SAL (μM)
Insulin/AMCA	45	66
Insulin/Cy2	119	294
Insulin/Cy3	213	272
Lectin-FITC	129	150
Collagen IV/Cy5	111	209
α-SMA/Alexa Fluor®488	256	130
α-SMA/Alexa Fluor®647	164	210
Hoechst 33342	130	100

GL: Glycerol Based Mountant; SAL: Methyl Salicylate Mountant.

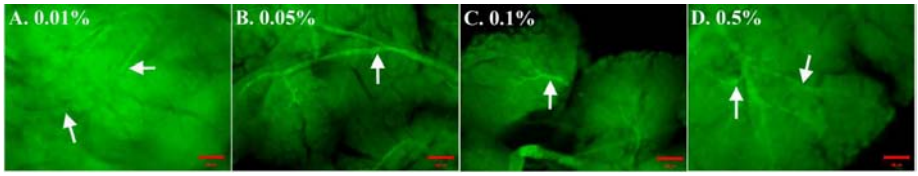

Figure 1: Determining the effect of different TX-100 concentrations on signal to background staining in pancreas whole-mounts. **(**A) and (D): Poor contrast and structural clarity of the vasculature (arrows) shown after incubation in 0.01% and 0.5% TX-100. (B) and (C): Improved contrast of vasculature (arrows) after permeabilization in 0.05% and 0.1% TX-100 concentrations with the best signal and background in tissues incubated in 0.1% Tx-100 (C). Bar = 100μm for all images.

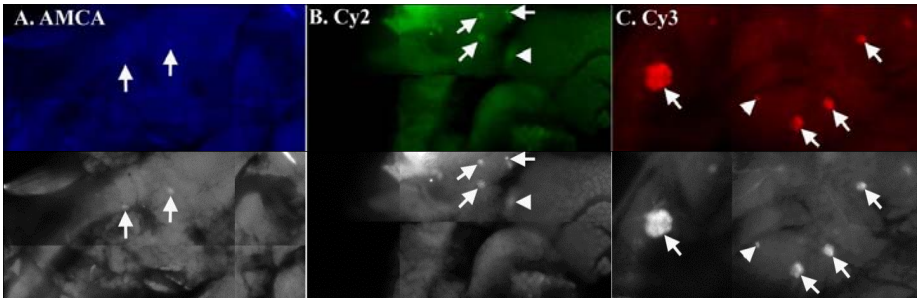

Figure 2: Pancreatic whole-mounts immunostained to reveal insulin (Ins) detected with AMCA (A), Cy2 (B) or Cy3 (C). Colour images shown are as those observed using the specific filter sets under wide-field epifluorescence microscopy. (A) Ins/AMCA stained islets (arrows) are barely detectable above background in GL or SAL (only SAL shown) as seen viewed by wide-field fluorescence microscopy. The grey-scale image shows AMCA-stained islets (arrows) more clearly but only after enhanced image contrast. (B) Cy2-stained islets (arrows) are detectable only when mounted in SAL (GL data not shown). Islets deep in the tissue are visible. (C) Islets are easily detectable (arrows) with Cy3 irrespective of mountant used (GL data shown). Arrowheads in Figures 2B & C indicate islets deep in the WMs.

antibody and mounting in either GL or SAL, signal to background contrast was not improved when viewed by WEM (comparative data not shown). Furthermore, the depth at which insulin/AMCA was detected by CLSM imaging remained markedly shallow compared to that of insulin/Cy2 or insulin/Cy3 (Table 4) (see below). In order to determine whether the blue emission was a problem in our tissues, we stained WMs with Hoechst 33342 and compared its detection limit to that of AMCA. Hoechst 33342 signals were detected significantly deeper than that of AMCA (Table 4) (see Discussion).

Because of the above limitations using insulin/AMCA, we investigated the use of anti-GP Cy2 and anti- GP Cy3 to detect insulin in WMs. Islets stained with insulin/Cy2 (in WMs mounted in GL) were barely visible against the high background when viewed by WEM (not shown), although the maximum depth observed by CLSM was significantly greater than in AMCA stained WMs (119μM vs 45μM; Table 4). In some cases insulin/Cy2 fluorescence was not detectable in the islet interior whereas the immunostained vasculature was clearly visible (Figure 3A). Furthermore, individual β-cells were only distinguishable in the more superficial Z-planes of islets (Figure 3A). By contrast, insulin/Cy2 signals were bright as seen in WEM (Figure 2B) and detected much deeper in WMs mounted in SAL compared to those mounted in GL (294μM vs 119μM); (Figure 3B, Table 4). Somewhat disappointing was a noticeable reduction in the clarity of signal (resolution) within 25μM–50μM from the surface although the signal intensity remained bright (Figure 3B).

On the other hand, signal intensity and structural resolution was markedly improved in WMs stained with insulin/Cy3, irrespective of the mounting medium (Figures 2C & Table 4). Viewed under WEM, islets were easily detectable and the signal to background fluorescence was much improved above that seen for Cy2 (Figures 2B & C). Islets were detected deep in the tissue (Table 4) and individual β-cells were distinguishable throughout the islet with minimal loss of signal in the deeper Z-planes (Figure 4). Other fluorophores in the green spectrum such as FITC and Alexa Fluor®488 were not assessed for insulin

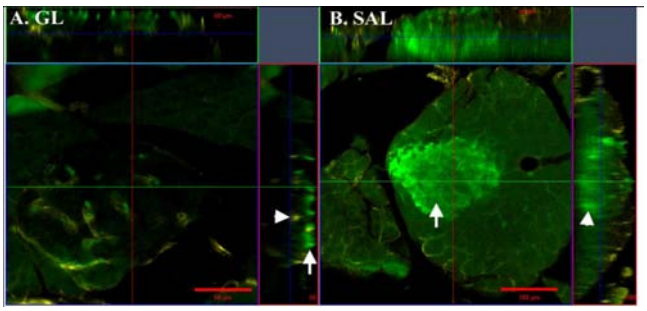

Figure 3: Orthogonal view of Z-stacks in whole-mounts stained with insulin/Cy2 + collagen IV/Cy5. The images shown in the X-Y planes are taken midway through the islets**.** (A) Insulin is only detected near the superficial plane of the whole-mount (arrow) in glycerol mountant (GL). This signal has virtually disappeared by midway through the islet whereas its vasculature stained with collagen IV/Cy5, is detectable throughout (arrowhead). Bar = 50μm and depth of Z-stack is 48μm. (B) Insulin staining (arrowhead) remains bright deep in tissues mounted in methyl salicylate (SAL). However, cellular resolution of insulin is poor (arrow) and the vasculature staining appears grainy. Bar = 100μm and depth of Z-stack is 112μm.

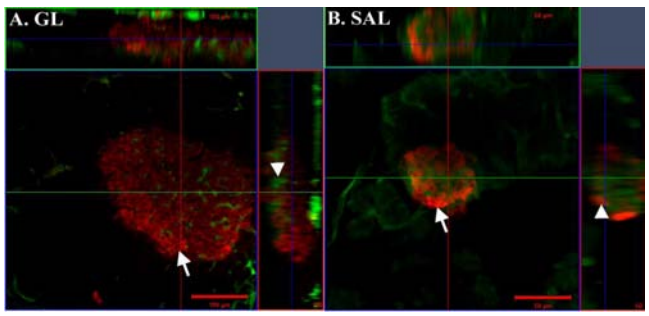

Figure 4: Orthogonal view of Z-stacks of pancreas whole-mounts stained with insulin/Cy3 + *Lycopersicon esculentum* Lectin-FITC. The images shown in the X-Y planes are taken midway through the islets**.** (A) Insulin signal is bright and detected with good resolution (individual β-cells can be identified) throughout a large islet in tissue mounted in glycerol (GL) (arrow). Vascular staining is also clearly preserved deep in the tissue (arrowhead). Bar = 100μm and depth of Z-stack is 108μm. (B) Insulin/Cy3 and Lectin-FITC are detected throughout the islet tissue mounted in methyl salicylate (SAL) (arrowhead indicates the Z-plane in which insulin and Lectin-FITC are detected) but the resolution of cellular staining (arrow) in the X-Y plane is reduced compared to that shown in Fig 4A. Bar = 50μm and depth of Z-stack is 52μm.

detection as we intended to use these for detecting the capillary bed and other antigens of interest to our study (not included here) in the WMs (Table 2).

Detection of the vasculature

Lectin-FITC demonstrated the vasculature to depths 120μM and 150μM in GL and SAL mountants respectively (Table 4), with the best resolution shown in GL. An alternative vascular marker (collagen IV/Cy5) was used in combination with insulin/Cy2 or insulin/Cy3. For the most part, the collagen IV/Cy5 signal was coincident with insulin at the deeper Z-planes (Table 4), but the resolution was poorer than that shown by Lectin-FITC in the deeper Z-planes. Vascular mural cells were easily detectable in the deeper Z-planes in both mountants (Table 4).

Discussion

With respect to the problems encountered with insulin/AMCA staining of our tissues, increasing AMCA-conjugated secondary antibody concentrations did not improve the signal. Furthermore, we also show that the poor AMCA staining was neither due to poor preservation of antigenicity nor to a low concentration of the primary antibody as insulin was readily detected using Cy2 and Cy3 conjugated secondary antibodies under the same staining conditions. We could exclude possible degradation of fluorophore antibody complex based on using a fresh batch of AMCA-conjugated secondary antibody.

The size of antibody conjugated fluorophores could prevent their entry into cells and thus reduce their detect ability. However, all the secondary antibodies used in our study were of similar size (≈150kDa) and WMs were well permeabilized. We observed that some primary/secondary antibody combinations (specifically Cy2-and Cy3-stained insulin) were detectable at ≈300μm, therefore theoretically these antibodies would only have to penetrate 150μM into the WM to fully saturate antigen binding sites of interest. We speculated that some internal absorption (excessive scattering of shorter blue emission wavelengths) may have occurred with AMCA fluorescence in these WMs. However, Hoechst 33342 signals were detected much deeper than AMCA, and since the peak emission is 10nm higher than that of AMCA, we hypothesized that this small increase in wavelength is enough to escape internal absorption properties of the tissue and hence is detectable deeper in the WM.

A likely reason for the difference in detection depths between AMCA and Hoechst (and other fluorophores) is that the AMCA molecule is highly polar compared to other fluorophores and thus may retard its permeability through cell membranes, particularly in WMs (personal communication). However, WMs had been exposed to methanol and TX-100 before staining and thus we would have expected lipid extraction to be sufficient to not retard the AMCA-antibody complex this severely. Although not part of this study, we would consider using other fluorophores such as Alexa Fluor®350 as a suitable option for viewing insulin in the blue spectrum.

The intense fluorescence of the cyanine dyes was beneficial for locating islets in WMs, particularly in SAL-mounted tissues. These dyes are known to be more efficient in a non-polar environment, and anti-fades (DABCO) are reported to reduce signal intensity [15]. The mounting medium is critical, since its polarity and pH can play a major role in fluorophore efficiency [15]. We performed a preliminary investigation into mountants incorporating urea (based on the Scale method) [16] without improvement in tissue clearing. Focus Clear™ is reported to clarify mouse pancreas [17] but it is extremely expensive and therefore currently not feasible for use in our research at this time.

Whilst both Cy2 and Cy3 provided brighter and detectable from deeper Z-planes in SAL-mounted WMs (Table 4), in our hands these fluorophores are limited for use in islet quantitation due to loss of structural resolution in the deeper planes in SAL. In GL mounts, Cy3 was the superior fluorophore for detecting the morphology of β-cells throughout the islets. Although not included in this study for insulin staining, the satisfactory staining and depth of detection observed for mural cells stained with Alexa Fluor® 488, this fluorophore could be considered as a suitable option for islet detection by WEM if using other fluorophores to detect the vasculature.

Insulin content in β-cells could vary depending on the physiological needs. Our findings indicate that due to its brightness, Cy3 appears to be the most suitable for detecting intracellular antigens over a wider range of concentrations. Unlike Cy2 and Cy5, Cy3 is brighter and photo stable in an aqueous medium [13]. In addition, background fluorescence was lowest in the red channel and provided the best contrast between signal and background in our WMs.

Conclusion

Choosing the correct fluorophores in designing multi-immunofluorescence studies is essential to minimize crosstalk across barrier filters [18]. The chosen fluorophores should be detectable in the same Z-plane in order to distinguish spatial relationships between microanatomical or cellular structures. Our study shows that different fluorophores detecting the same structures have variable efficiencies, and thus must be carefully tested and selected at the start of any study to avoid misinterpretation of data. For our pancreatic tissues, AMCA was found to be the least suitable fluorophore due to the likelihood of a combination of it being a weak emitter, subject to internal absorption and possibly retarded penetration through cell membranes. The cyanine dyes and Alexa Fluor® dyes are clearly more superior for detecting antigens in the deeper planes of our WMs with Cy3 showing the best resolution of structures. Mounting WMs in GL or SAL affected signal detection and resolution quality differently. Cy2 and Cy5 performed better in detecting antigens located deep in SAL-mounted tissues and Cy3, Lectin-FITC, and Alexa Fluor® dyes offering improved resolution in GL-mounted tissues. Our study thus highlights the importance of choosing suitable fluorophores and mounting media for multi-immunofluorescence in deep tissue imaging particularly for studying heterogeneous tissues which may have different optical and internal scattering properties.

References

1. Chiu YC, Hua TE, Fu YY, Pasricha PJ, Tang SC. 3-D imaging and illustration of the perfusive mouse islet sympathetic innervation and its remodelling in injury. Diabetologia. 2012; 55: 3252-3261.
2. Juang JH, Peng SJ, Kuo CH, Tang SC. Three-dimensional islet graft histology: panoramic imaging of neural plasticity in sympathetic reinnervation of transplanted islets under the kidney capsule. Am. J. Physiol-Endoc. M. 2014; 306: E559-E570.
3. Juang JH, Kuo CH, Peng SJ, Tang SC. 3-D Imaging Reveals Participation of Donor Islet Schwann Cells and Pericytes in Islet Transplantation and Graft Neurovascular Regeneration. E Bio Medicine. 2015; 2: 109-119.
4. Reinert RB, Cai Q, Hong JY, Prank JL, Aamodt K, Prasad N, et al. Vascular endothelial growth factor coordinates islet innervation via vascular scaffolding. Development. 2014; 141: 1480-1491.
5. Rodriguez-Diaz R, Abdulreda MH, Formoso AL, Gans I, Ricordi C, Berggren PO, Caicedo A. Innervation patterns of autonomic axons in the human endocrine pancreas. Cell Metab. 2011; 14: 45-54.
6. Rodriguez-Diaz R, Caicedo A. Neural control of the endocrine pancreas. Best Pract Res Clin Endocrinol Metab. 2014; 28: 745-756.
7. Tang SC, Chiu YC, Hsu CT, Peng SJ, Fu YY. Plasticity of Schwann cells and pericytes in response to islet injury in mice. Diabetologia. 2013; 56: 2424-2434.
8. Tang SC, Peng SJ, Chien HJ. Imaging of the islet neural network. Diabetes Obes Metab. 2014; 16 Suppl 1: 77-86.
9. El-Gohary Y, Tulachan S, Branca M, Sims-Lucas S, Guo P, Prasadan K, ChiyoShiota, et al. Whole-Mount Imaging Demonstrates Hypervascularity of the Pancreatic Ducts and Other Pancreatic Structures. The Anat. Rec. 2012; 295: 465-473.
10. Jamur MC, Oliver C. Permeabilization of cell membranes. Jamur MC, Oliver C, editors. In: Immunocytochemical methods and protocols. Humana Press, 2010; 63-66.
11. Krenacs T, Krenacs L, Raffeld M. Multiple Antigen Immunostaining Procedures. Jamur MC, Oliver C, editors. In: Immunocytochemical methods and protocols. Humana Press, 2010; 281-300.
12. Tsien RY, Waggoner A. Fluorophores for confocal microscopy. Pawley JB, editor. In: Handbook of biological confocal microscopy. Springer US, 1995; 267-279.
13. Shaner NC, Steinbach PA, Tsien RY. A guide to choosing fluorescent proteins. Nat Methods. 2005; 2: 905-909.
14. Richardson DS, Lichtman JW. Clarifying Tissue Clearing. Cell. 2015; 162: 246-257.
15. LonginA, Souchier C, Ffrench M, Bryon PA. Comparison of anti-fading agents used in fluorescence microscopy: image analysis and laser confocal microscopy study. J. Histochem. Cytochem. 1993; 41: 1833-1840.
16. Hama H, Kurokawa H, Kawano H, Ando R, Shimogori T, Noda H, et al. Scale: a chemical approach for fluorescence imaging and reconstruction of transparent mouse brain. Nat Neurosci. 2011; 14: 1481-1488.
17. Fu YY, Lu CH, Lin CW, Juang JH, Enikolopov G, Sibley E, et al. Three-dimensional optical method for integrated visualization of mouse islet microstructure and vascular network with subcellular-level resolution. J. Biomed. Opt. 2010; 15: 046018-046018.
18. Hale IL, Matsumoto B. Resolution of Sub cellular Detail in Thick Tissue Sections: Immunohistochemical Preparation and Fluorescence Confocal Microscopy. Matsumoto B, editor. In: Cell biological applications of confocal microscopy. Academic Press, 2003; 301-335.

J Mol Biol & Mol Imaging - Volume 2 Issue 2 - 2015
ISSN : 2471-0237 | www.austinpublishinggroup.com

Citation: Naidoo V, Lang DM and Van der Merwe EL. Addressing the Challenges of Multi-Immunofluorescent Deep Tissue Imaging of Islets and Vasculature in the Rat Pancreas. J Mol Biol & Mol Imaging. 2015; 2(2): 1022.